Universality classes for wetting in two-dimensional random-bond systems

Joachim Wuttke
Institut Laue-Langevin, 156X, 38042 Grenoble CEDEX 9, France
and Institut für Physikalische Chemie, Universität Mainz, Jakob-Welder-Weg 15, 6500 Mainz, Germany

Reinhard Lipowsky
Institut für Festkörperforschung, Forschungszentrum Jülich, Postfach 1913, 5170 Jülich, Germany
(Received 27 February 1991; revised manuscript received 28 June 1991)

Interface-unbinding transitions, such as those arising in wetting phenomena, are studied in two-dimensional systems with quenched random impurities and general interactions. Three distinct universality classes or scaling regimes are investigated using scaling arguments and extensive transfer-matrix calculations. Both the critical exponents and the critical amplitudes are determined for the weak- and the strong-fluctuation regime. In the borderline case of the intermediate-fluctuation regime, the asymptotic regime is not accessible to numerical simulations. We also find strong evidence for a nontrivial delocalization transition of an interface that is pinned to a line of defects.

I. INTRODUCTION

Interfacial wetting phenomena in random systems have been studied recently by scaling arguments,[1,2] replica calculations,[3] and renormalization-group arguments.[4] Various types of universal behavior have been predicted for the singularities at critical wetting transitions. In the work reported here, we show that both the critical exponents and the critical amplitudes can be determined by scaling arguments. We test all predictions by extensive numerical calculations for a two-dimensional random-bond lattice model. We discuss the conditions under which this model can be used to simulate a continuum.

As usual, the growth of thickening of a wetting layer will be described as the unbinding of an interface from a hard wall. Two types of effective interactions act on the interface at a separation l from the wall: A direct interaction $V_0(l)$ which arises from the microscopic forces between the molecules or atoms, and a fluctuation-induced interaction $V_{\rm fl}(l)$ which arises from the roughness of the interface and includes the effect of the quenched randomness. From scaling arguments, one estimates $V_{\rm fl}(l)\sim l^{-\tau}$ for large l. The decay exponent is found to be $\tau=2$ for thermal fluctuations in a pure system, and $\tau=1$ in random-bond systems.

The competition between V_0 and $V_{\rm fl}$ leads to various scaling regimes.[1] Apart from a mean-field regime, it has been predicted that there are three regimes in which the critical behavior is governed by interface fluctuations: a weak-fluctuation (WFL) regime, a strong-fluctuation (SFL) regime, and an intermediate-fluctuation (IFL) regime with various subregimes for the borderline case $V_{\rm fl}\sim V_0$. In this paper, we will study the distinct critical behavior within these three scaling regimes.

Our paper is organized as follows. After introducing the effective interface Hamiltonian in Sec. II, we collect in Sec. III all known results about the scaling of a free interface. A derivation of these relations for general dimension is given in Appendix A. In Sec. IV, the scaling relations are applied to an interface subject to a long-range potential with $V_0\sim l^{s}$ for large l. Apart from the critical exponents, we also determine the critical amplitudes. Thus we obtain a fairly complete description of the WFL regime. The IFL regime with $s=-\tau$ is discussed in Sec. V. In Sec. VI, the transfer matrix is introduced in order to describe the system by a partial differential equation of the Schrödinger type. The validity of this equation for a lattice model is studied in Appendix B. This Schrödinger equation can be solved by a replica ansatz for the simplest short-range potential, i.e., for a square well.[3] In Sec. VII, the behavior of an interface in this potential is studied as an example for the SFL regime. Again, scaling arguments are used to determine the parameter dependence of the critical amplitudes. Finally, in Sec. VIII, we study a closely related problem, the unbinding of an interface from a symmetric square-well potential, without a hard wall at $l=0$.

For all scaling regimes, extensive numerical simulations have been performed. For different strengths of the direct interaction $V_0(l)$ and of the random potential $V_r(x,l)$, a relaxation of $V_r(x,l)$ is generated and then the transfer-matrix technique is used to calculate the interface configuration $l(x)$. The mean interface separation $\bar{l}$ is obtained as the average over $l(x)$. A precise definition of $\bar{l}$ for different boundary conditions is given in Appendix C. Although we consider only two-dimensional systems, the simulations are extremely time consuming. In Appendix C we estimate that the calculation time which is needed to obtain a value $\bar{l}$ with a given precision is approximately proportional to $\bar{l}^{5/2}$. This rather strong dependence restricts the numerically accessible range of the critical region. In practice, we controlled the error by monitoring the convergence of $\bar{l}$ by succesively averaging over configurations of increasing length. We retained

only those data points for which $\bar{l}$ became stable within 3% limits.

II. INTERFACE HAMILTONIAN

To proceed, let x be the longitudinal coordinate, and describe the fluctuating interface by its distance $l(x)$ from the wall. As usual, only interface configurations without overhangs will be taken into account. The effective Hamiltonian $\mathcal{H}$ then has the form

$$\mathcal{H}\{l(x)\}=\int dx \left[\frac{\tilde{\Sigma}}{2}[\nabla l(x)]^2+V_r(x,l(x)) + V_0(l(x)) \right], \quad (1)$$

where $\tilde{\Sigma}$ is the effective interface stiffness.

The random potential $V_r(x,l)$ describes the effect of quenched impurities. It is assumed to be Gaussian distributed and short-range correlated according to

$$\langle V_r(x,l)V_r(x',l')\rangle=2D\delta_{a_\parallel}(x-x')\delta_{a_\perp}(l-l') , \quad (2)$$

where δ_a denotes a smeared-out δ function of width a. A lattice version of this Hamiltonian corresponds to an Ising model with random-bond disorder. Note that for $D=0$, the interfacial stiffness in an Ising model diverges in the limit of zero T.[5,6]

Finally, the external potential $V_0(l)$ describes the direct interaction between the interface and the hard wall at $l=0$. In the case of complete wetting, it is given by $V_0(l)=hl$, where h is the difference in chemical potential between the wetting layer and the bulk phase separated by the interface. For the case of critical wetting, V_0 is determined by molecular interactions between the different phases.[7]

If $V_0(l)$ contains repulsive and attractive components that are both long ranged, we are in the mean-field regime and $\bar{l}$ may be determined by minimizing $V_0(\bar{l})$. In this case, the effect of fluctuations can be calculated by perturbation theory.[7]

Here, we focus on the different fluctuation regimes and take the repulsive component $V_R(l)$ of $V_0(l)$ to be a hard wall with

$$V_R(l)=\begin{cases}\infty & \text{for } l\le 0\\ 0 & \text{for } l>0 .\end{cases} \quad (3)$$

In our numerical simulations at $T=0$, the interface configuration has been calculated in the random-bond Ising model corresponding to the continuum model (1) and (2). As explained in Appendix C, both models are equivalent as long as the interface fluctuations are weak.

III. SCALING OF A FREE INTERFACE

To assess the scaling behavior of the involved quantities, we first consider a free interface with $V_0=0$. The results will then be applied to an interface in a long-ranged potential V_0.

An interface segment of longitudinal dimension $L_\perp$ has, on average, a transverse dimension

$$L_\perp\approx l_0^{1-\zeta}L_\parallel^{\zeta} . \quad (4)$$

For the present discussion, it is not necessary to give a more precise description based on the difference correlation function. The roughness exponent ζ is $\zeta=\frac{1}{2}$ for thermally excited fluctuations; for random-bond systems it has been shown to be $\zeta=\frac{2}{3}$.[8,9] The relation (4) indicates that longitudinal and transverse lengths show different behavior under a rescaling of the system. If we assume that the reduced Hamiltonian $\mathcal{H}\{l\}/T$ is invariant under the rescaling

$$x\to x/b \quad \text{and} \quad l\to l/b^{\zeta} , \quad (5)$$

we can determine the scaling dimension of the quantities involved in $\mathcal{H}$. In Appendix A, we show how the amplitude l_0 is then obtained as a function of T, $\tilde{\Sigma}$, D, and $a_\perp$.

For thermal fluctuations, one has $l_0=f_{\rm th}T/\tilde{\Sigma}$, where $f_{\rm th}$ is a dimensionless constant. For random-bond disorder, Nattermann and Renz[10] found the scaling form

$$l_0=(D/\tilde{\Sigma}T)f(T^3/a_\perp D\tilde{\Sigma}) . \quad (6)$$

The asymptotic behavior of the function $f(x)$ is known: for $T\to 0$, fluctuations are driven by the random potential only, and the amplitude l_0 must be independent of T; for high temperatures, on the other hand, the interface position is given by a broad distribution, and l_0 is independent of $a_\perp$. Thus one obtains

$$f(x)\approx\begin{cases}f_0 x^{1/3} & \text{for small } x\\ f_\infty & \text{for large } x .\end{cases} \quad (7)$$

Here f_0 and f_∞ are two dimensionless coefficients.

These results shall now be used to discuss the scaling behavior of an interface in an external potential $V_0(l)$. If the potential binds the interface with a mean distance $\bar{l}$ to the wall, it also restricts fluctuations of the interface to a range $L_\perp\lesssim\xi_\perp$. The corresponding longitudinal length of the largest fluctuation is the correlation length $\xi_\parallel$. We assume (4) to remain valid on all scales up to $L_\parallel\lesssim\xi_\parallel$, $L_\perp\lesssim\xi_\perp$, so that we have

$$\xi_\perp\approx c l_0^{1-\zeta}\xi_\parallel^{\zeta} , \quad (8)$$

where c is a coefficient of order one.

On larger scales $L_\parallel\gg\xi_\parallel$; however, where $L_\perp$ is bound by $\xi_\perp$, the interface is essentially flat. This may be seen as an elimination of capillary modes by the external potential $V_0(l)$. The corresponding loss in free energy can be described as a fluctuation-induced potential $V_{\rm fl}(\xi_\perp)$. The different contributions to $V_{\rm fl}$ stem from the elastic energy, the entropy loss, and the random potential.

The elastic energy can be estimated as

$$V_\nabla(\xi_\perp)\sim\tilde{\Sigma}(\nabla l)^2\sim\tilde{\Sigma}(\xi_\perp/\xi_\parallel)^2\sim\tilde{\Sigma}l_0^{\tau}\xi_\perp^{-\tau} , \quad (9)$$

with a decay exponent $\tau\equiv 2(1-\zeta)/\zeta$. For thermal fluctuations one has $\tau=2$ in $d=1+1$, and the entropy loss $-T\Delta s$ is of the same order as $V_\nabla(\xi_\perp)$.[1] In the presence of the random potential with $\tau=1$ in $d=1+1$, *entropy*

effects become irrelevant. Instead, the interface makes transverse excursions in order to lower its *energy*. This energy gain must overcome the elastic energy. So the random potential is expected to give a contribution ΔV of the order of $V_\nabla(\xi_\perp)$.

Hence the fluctuation-induced potential is

$$V_{\rm fl}(\xi_\perp)\sim\tilde{\Sigma}l_0^{\tau}\xi_\perp^{-\tau} \tag{10}$$

for both thermal fluctuations and random-bond disorder.

IV. WEAK-FLUCTUATION REGIME

Using these results, we will now determine the behavior of an interface in a potential that is given by a power law $V_0\sim l^s$. A suitable parametrization is

$$V_0(l)=\begin{cases}\infty & \text{for } l<0\\ w[l+a_\perp)^s-a_\perp^s]/s & \text{for } l\geq 0\ .\end{cases} \tag{11}$$

Here we have introduced the lattice constant $a_\perp$ as a cutoff at small l, in order to allow for exponents $s<0$. Furthermore, we have chosen a form that has an analytic continuation in the limit of zero s.

In the weak-fluctuation regime, interface fluctuations are of the same order as the mean distance between the interface and the wall, $\xi_\perp\approx\bar{l}$. So we may estimate the total free energy as

$$V_{\rm tot}(\bar{l})\approx V_{\rm fl}(\bar{l})+V_0(\bar{l})\ , \tag{12}$$

and by minimizing $V_{\rm tot}$ we obtain for $\bar{l}\gg a_\perp$ the asymptotic result

$$\bar{l}\approx(w/\tau\tilde{\Sigma}\bar{l}_0^{\tau})^{-\psi}\ \text{ with }\ \psi=1/(\tau+s)\ . \tag{13}$$

As this relation has been obtained from (4) through various rough estimates, we replaced l_0 by $\bar{l}_0$ to account for any prefactor. Also, $\bar{l}_0$ will be different for different functions $V_0(l)$. The scaling forms for $\bar{l}_0$ are completely analogous to those for l_0: For thermal fluctuations, we have $\bar{l}_0=\bar{f}_{\rm th}T/\tilde{\Sigma}$, and in the presence of the random potential $\bar{l}_0=(D/\tilde{\Sigma}T)\bar{f}(T^3/a_\perp D\tilde{\Sigma})$ with the two limiting cases

$$\bar{f}(x)\approx\begin{cases}\bar{f}_0x^{1/3} & \text{for small } x\\ \bar{f}_\infty & \text{for large } x\ .\end{cases} \tag{14}$$

As a numerical test of (13), we consider first the case that corresponds to complete wetting, $s=1$. The behavior $\bar{l}\sim w^{-\psi}$ with $\psi=\frac{1}{2}$ has already been confirmed at $T=0$.[11] Here we report simulation results for $T>0$. With our choice $T=0.15$ we are clearly in the low-temperature regime, where $\bar{l}_0$ can be estimated as

$$\bar{l}_0\simeq\bar{f}_0D^{2/3}/\tilde{\Sigma}^{4/3}a_\perp^{1/3}\ . \tag{15}$$

In our simulations, $\bar{l}$ has been measured as a function of w at three different values of D. In Fig. 1, the data are combined into a double logarithmic plot which shows the interfacial separation $\bar{l}$ against the rescaled potential strength $w/D^{2/3}$. The data collapse onto one curve which confirms the scaling of w and D over two decades in D. For small $\bar{l}$, there are clearly lattice effects. For

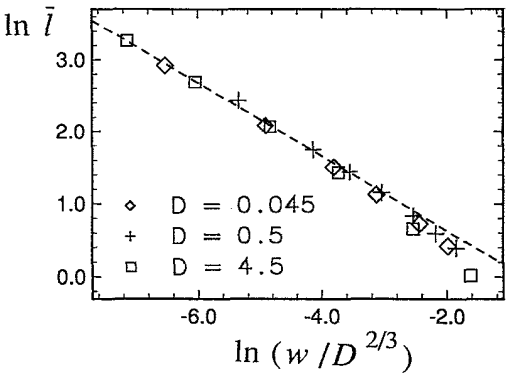

FIG. 1. Interfacial separation $\bar{l}$ for the potential $V_0(l)=w(l-a_\perp)$ at $T=0.15$ for different values of the disorder strength D. The data are scaled in order to test the scaling prediction $\bar{l}\sim(w/D^{2/3})^{-\psi}$. The line corresponds to $\psi=0.511$, as found by a fit to the data with $\bar{l}>3.5a_\perp$. Here, as in all the figures, units of $a_\perp=\tilde{\Sigma}/2=1$ are used.

$\bar{l}\gtrsim a_\perp$, on the other hand, the data fall onto a line, the slope of which is just the exponent ψ. In order to determine the value of ψ and its error, we have fitted a line to those data for which $\bar{l}>a_1$, with different cutoffs a_1 in the range from $2a_\perp$ to $7a_\perp$. Thereby we find $\psi=0.51\pm0.02$, which agrees quite well with the predicted $\psi=\frac{1}{2}$. For the prefactor we obtain $\bar{f}_0\simeq0.64\pm0.13$. In all the simulations, lengths and potential strengths have been measured in units of $a_\perp=\tilde{\Sigma}/2=1$.

Next, we consider the case $s=0$, where the potential (11) is replaced by its analytic continuation

$$V_0(l)=\begin{cases}\infty & \text{for } l<0\\ w\ln[(l+a_\perp)/a_\perp] & \text{for } l\geq 0\ .\end{cases} \tag{16}$$

As there is a slight advantage in calculation speed, we performed the corresponding simulations at $T=0$. As shown in Fig. 2, the data collapse again for three different

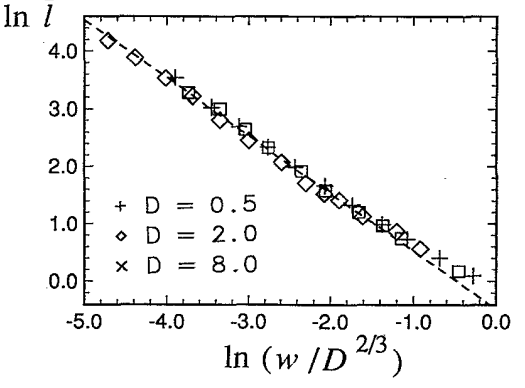

FIG. 2. Interfacial separation $\bar{l}$ for the potential $V_0(l)=w\ln(l/a_\perp-1)$ at $T=0$ for different D. The dashed line corresponds to $\bar{l}\sim(w/D^{2/3})^{-\psi}$ with an exponent $\psi=1.00$, as found by a fit to the data with $\bar{l}>4.5a_\perp$.

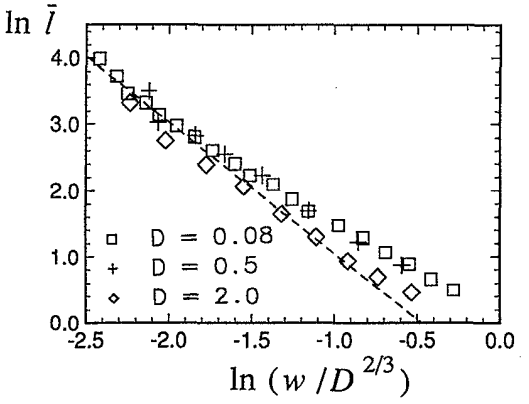

FIG. 3. Interfacial separation $\bar{l}$ for the potential $V_0(l)=w(l^s-a_\perp^s)/s$ with $s=-0.5$. The dashed line corresponds to the asymptotic scaling prediction $\bar{l}\sim(w/D^{2/3})^{-\psi}$; the exponent $\psi=1.98$ was found by a fit to the data with $\bar{l}>14a_\perp$.

values of D. Asymptotically, the scaling prediction $\bar{l}\sim(w/D^{2/3})^{-\psi}$ can be confirmed. As before, the exponent can be determined with different cutoffs $\bar{l}>a_\perp$, and is found to be $\psi=0.99\pm0.02$, in agreement with the predicted $\psi=1$. The prefactor is $\bar{f}_0\simeq0.81\pm0.04$. A closer agreement with the value of $\bar{f}_0$ for the case $s=1$ is not expected because the derivation of (13) implied that $\bar{f}_0$ may be different by a factor of $O(1)$ for different potentials $V_0(l)$.

The scaling result (13) should remain valid for negative exponents s as long as $s>-\tau$. By numerical simulations it is, however, quite difficult to verify (13). In Fig. 3 we show results for $s=-0.5$. The collapse of the data for different D is poor, and the asymptotic regime has presumably not been reached. By the same fitting procedure as used before, we find $\psi=2.1\pm0.3$, which is compatible with the prediction $\psi=2$, although it is much less significant than the results for $s=1$ and 0. For the prefactor, one finds $\bar{f}_0=0.63\pm0.22$.

V. INTERMEDIATE-FLUCTUATION REGIME

On the borderline between the WFL regime and the SFL regime, Lipowsky and Nieuwenhuizen[12] found for thermal fluctuations an intermediate-fluctuation (IFL) regime with some interesting features, resulting from the competition between $V_{\text{fl}}(l)$ and the long-range part of $V_0(l)$. In this case, the short-range part of V_0 may play a crucial role. To study this effect, we introduce another parameter $V_0(0)=-u$ instead of the cutoff used in (11), and define the potential by

$$V_0(l)=\begin{cases}\infty & \text{for } l<0\\ -u & \text{for } 0\le l<a_\perp\\ -w/l^\tau & \text{for } a_\perp\le 0\ .\end{cases} \tag{17}$$

For thermal fluctuations with $D=0$ and $\tau=2$, one finds three different subregimes: If u is below a critical value u_{cm}, $\bar{l}$ behaves as an essential singularity,

$$\bar{l}\sim\exp\left[4\pi\left[\frac{w_c}{w-w_c}\right]^{1/2}\right] \quad \text{with } w_c=T^2/8\tilde{\Sigma}\ , \tag{18}$$

and is independent of u (subregime A). For $u>u_{\text{cm}}$, on the other hand, one has a power law

$$\bar{l}\sim(u-u_c)^{-\psi}\ , \tag{19}$$

where not only u_c, but also the exponent ψ depends on w [subregimes B and C, with two different functions $\psi(w)$].

It has been suggested that a random-bond system should show qualitatively the same behavior when the exponent in the potential (17) is $\tau=1$.[4] Again, it proved impossible to verify or to falsify this prediction numerically.

In Figs. 4–6, we report a series of simulations at $T=0$ for $D=4.5$. Figure 4 shows $\bar{l}$ as a function of w at different values of u, fitted as an essential singularity

$$\bar{l}\approx\mathcal{A}\exp\left[\gamma\left[\frac{w_c}{w-w_c}\right]^{1/2}\right]\ . \tag{20}$$

At $u=1.4$, we find $w_c<0$, indicating that we are outside sugregime A. The other three curves depend only weakly on u, and are compatible with (20). For the prefactor in the exponent, we obtain $\gamma=5.2\pm0.2$; other simulations indicate that γ should depend on D. However, as demonstrated in Fig. 5, the data shown in Fig. 4 may also be fitted by a power law

$$\bar{l}\approx\mathcal{A}[(w-w_c)/w_c]^{-\psi}\ . \tag{21}$$

Therefore, on the basis of the available data, a subregime A described by (20) cannot be confirmed.

As a test of (19), $\bar{l}$ has been calculated as a function of u at different values of w; see Fig. 6. The data are well

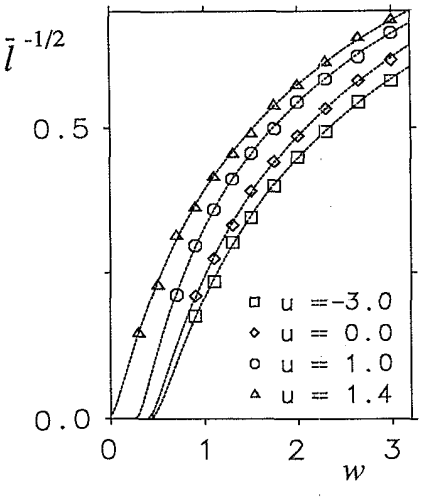

FIG. 4. Intermediate-fluctuation regime. The interface in the potential as given by (17) for $T=0$, $D=4.5$, and different u. The dashed lines represent a fit of $\bar{l}(w)$ in terms of an essential singularity; see (20).

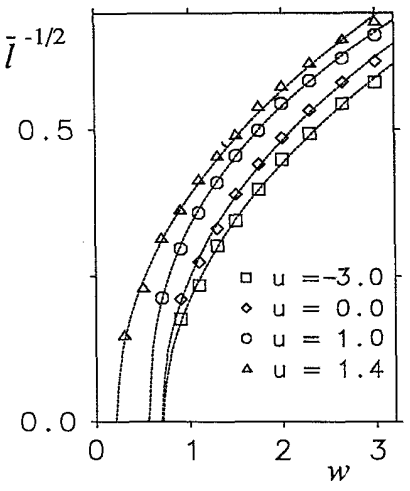

FIG. 5. The same data as in Fig. 4, but fitted to a power law $\bar{l}\sim(w-w_c)^{-\psi}$. For the effective exponent, one finds $\psi_{\text{eff}}=1.65\pm0.25$.

fitted by a power law

$$\bar{l}\approx\mathcal{A}[u-u_c(w)]^{-\psi} \quad \text{with } \psi=2\ ; \tag{22}$$

thus the dependence of ψ on w could not be verified. It is, however, unlikely that the data shown in Fig. 6 belong already to the asymptotic range $\bar{l}\gg a_\perp$ for which (19) should be valid. This is evident from the behavior for $w=0.6$, where $\bar{l}$ is well described by (22) until it attains a finite value at $\bar{l}\simeq 100$.

VI. TRANSFER MATRIX AND SCHRÖDINGER EQUATION

Our discussion of the SFL regime is based on an analytic result found by a replica ansatz. Therefore, at this point we have to introduce the transfer-matrix method. For the application of this formalism, we have to discretize the model in the horizontal direction, so that the

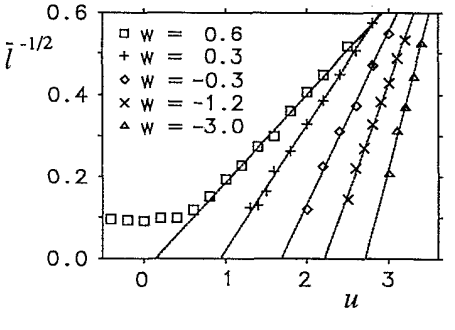

FIG. 6. Dependence of the interfacial separation $\bar{l}$ on the short-range part $V_0(0)=-u$ of the potential (17), for $T=0$, $D=4.5$, and different w. The dashed lines represent the functional dependence $\bar{l}\sim(u-u_c)^{-2}$. The asymptotic behavior of $\bar{l}$ is, however, not accessible, as is evident for $w=0.6$.

Hamiltonian (1) decomposes as

$$\mathcal{H}\{l\}=\sum_x \Delta x H_x(l(x+\Delta x),l(x))\ , \tag{23}$$

with

$$H_x(l',l)=\frac{\tilde{\Sigma}}{2}\left[\frac{l'-l}{\Delta x}\right]^2+V(x,l)\ ,$$
$$V(x,l)=V_r(x,l)+V_0(l)\ . \tag{24}$$

The weight $W(x,l)$ of a path ending at (x,l) satisfies the equation

$$W(x+\Delta x,l)=\mathcal{N}^{-1}\int dl' \exp\left[-\frac{\Delta x H_x(l,l')}{T}\right]W(x,l')\ , \tag{25}$$

where $\mathcal{N}$ is an arbitrary normalization constant. The integral kernel in (25) is called the transfer matrix. In the limit of infinitesimal Δx, an expansion of (25) leads to a differential equation of the Schrödinger type. All attempts to find analytic expressions for $W(x,l)$ are based on this Schrödinger equation. Numerical implementations of (25), however, use a discrete lattice with finite Δx for which the integral $\int dl'$ is repalced by a sum $\sum_{l'}\Delta l$. To find out under which conditions the analytic expression might be valid for finite Δx and Δl, we review the derivation of the differential equation in Appendix B.

We find that one has to require

$$|V(x,l)|\Delta x/T\ll 1\ , \tag{26}$$

and, in addition, one of the two inequalities

$$\Delta l\ll(T\Delta x/\tilde{\Sigma})^{1/2}\ll\xi_\perp \quad \text{for case (i)}\ ,$$
$$(T\Delta x/\tilde{\Sigma})^{1/2}\ll\Delta l\ll\xi_\perp \quad \text{for case (ii)}\ . \tag{27}$$

Under these conditions we can write (25) as the Schrödinger-type equation given by

$$\frac{\partial}{\partial x}W_x(l)=-\frac{\hat{H}(x,l)}{T}W_x(l)\ , \tag{28}$$

with the Hamilton operator

$$\hat{H}(x,l)\equiv V(x,l)-\Gamma\frac{\partial^2}{\partial l^2}\ . \tag{29}$$

For the coefficient Γ, one obtains

$$\Gamma=\begin{cases}\dfrac{T^2}{2\tilde{\Sigma}} & \text{for case (i)}\\ \dfrac{T\Delta l^2}{\Delta x}\exp\left[-\dfrac{\tilde{\Sigma}(\Delta l)^2}{2T\Delta x}\right] & \text{for case (ii)}\ ,\end{cases} \tag{30}$$

where the cases (i) and (ii) are given by the corresponding condition in (27).

Note that condition (i) is automatically satisfied in the continuum limit, with infinitesimal $\Delta x\sim\Delta l$. In a numerical simulation, however, $\xi_\perp/\Delta l$ is restricted by the finite size of the system, and it is easier to fulfill condition (ii) by an appropriate choice of T.

VII. STRONG-FLUCTUATION REGIME

By analogy with the case of thermal fluctuations, we expect the strong-fluctuation regime to display universal behavior for all potentials that are more short ranged than $V_{\text{fl}}(l)$. Here we study the simplest short-range potential, a square well given by

$$V_0(l)=\begin{cases}\infty & \text{for } l<0\\ -u & \text{for } 0\le l<a_V\\ 0 & \text{for } a_V\le l\ .\end{cases} \tag{31}$$

In the absence of random impurities ($D=0$), this potential allows for an indirect test of the validity of (28) for discrete systems. There exists a well-known solution of the stationary Schrödinger equation that yields for $\bar{l}\gg a_V$

$$\bar{l}\approx\left[\frac{u-u_0}{u_0}\right]^{-1},\quad u_0(T)=\frac{\pi^2}{4}\frac{T}{a_V^2}\ . \tag{32}$$

For $u\simeq u_0$, condition (26) takes the form

$$\Gamma\Delta x/Ta_V^2\ll 1\ . \tag{33}$$

In the limiting case (ii) as given by (30), this reduces to

$$\Delta l^2\exp[-\tilde{\Sigma}(\Delta l)^2/2T\Delta x]\ll a_V^2\ . \tag{34}$$

In this case, we may choose $a_V=\Delta l$, since the inequality in (27) assures that the exponential factor is small compared to one. In the limiting case (i), on the other hand, one has $\Gamma=T^2/2\tilde{\Sigma}$, and a combination of (33) and (27) yields

$$\Delta l\ll(T\Delta x/\tilde{\Sigma})^{1/2}\ll a_V\ . \tag{35}$$

Furthermore, the asymptotic Schrödinger equation result (32) is valid only if $a_V\ll\bar{l}$. These conditions are satisfied in the continuum limit, but are almost impossible to realize in a numerical simulation, where we are restricted to $\bar{l}\lesssim 100\Delta l$. In order to vary $\bar{l}$ over at least two decades, we have to choose $a_V=\Delta l$.

This conclusion has been confirmed by numerical calculations with $D=0$; see Fig. 7. At different T, $\bar{l}$ has been determined as a function of u. Since no average over random distributions is involved, these numerical data are very accurate. We confirm the probability $\bar{l}\sim(u-u_0)^{-1}$, and obtain by extrapolation the critical potential strength u_0. In Fig. 7, these values for u_0 are plotted against T. For low temperatures, $T\lesssim 1$, we find $u_0\sim\Gamma$, with Γ as given by (30) case (ii). The high-temperature case (i), with $\Gamma\sim T^2$, on the other hand, is not accessible because our choice $a_V=\Delta l$ violates condition (35). Thus we conclude that the continuum model, described by the Schrödinger equation (28) and case (ii) for Γ, can accurately be simulated on a discrete lattice as long as we work at sufficiently low temperatures.

We now come back to the case of random-bond disorder. By a replica ansatz, Kardar[3] obtained for the well

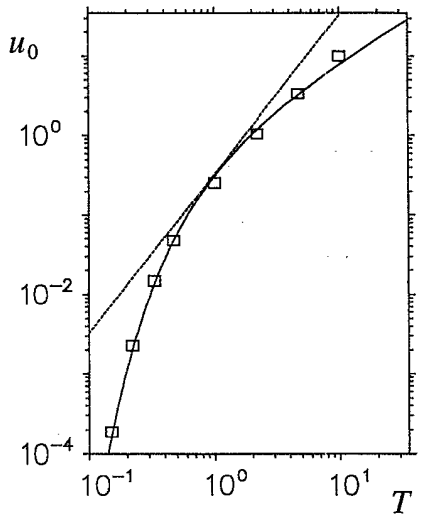

FIG. 7. Critical potential strength u_0 for unbinding by thermal fluctuations ($V_r=0$) from a square-well potential as in (31) with $a_V=\Delta l$. In the low-temperature range, $u_0\simeq 0.85T\exp(-1/T)$ (solid lines), whereas the high-temperature behavior $u_0\sim T^2$ (dashed line) is not accessible.

potential (31) in the presence of a random potential the behavior

$$\bar{l}\approx\frac{Du_0}{T}(u-u_c)^{-2}\ \text{ with }\ u_c(D,T)=u_0+\frac{D}{a_VT}\ . \tag{36}$$

Both equations show spurious singularities at small T. It seems that these divergences are due to the neglect of the finite width of the random potential correlation as in (2). There is no obvious way to include such a finite width in the replica formalism.

We can, however, go back to the scaling arguments presented in Sec. III, and use the scaling function (6) for a generalization of (36). As in Sec. IV, we introduce a new notation,

$$\hat{l}_0\equiv(D/\tilde{\Sigma}T)\hat{f}(T^3/a_\perp D\tilde{\Sigma})\ , \tag{37}$$

in order to account for different prefactors. We replace D/T by the general form $\hat{l}_0\tilde{\Sigma}/\hat{f}_\infty$ and substitute u_c for u_0 in the amplitude of $\bar{l}$. So we conjecture that the full description of the interfacial behavior is given by the scaling form

$$\bar{l}\approx\frac{Du_c}{T\hat{f}_\infty}\hat{f}(T^3/D\tilde{\Sigma}a_\perp)(u-u_c)^{-2}\ , \tag{38}$$

with

$$u_c(D,T)\approx u_0+\frac{D}{a_VT\hat{f}_\infty}\hat{f}(T^3/D\tilde{\Sigma}a_\perp)\ . \tag{39}$$

For large T, these relations contain the replica result (36) since $\hat{f}(x)\approx\hat{f}_\infty$ for large x. For small T, u_0 as given by (32) goes rapidly to zero due to the exponential factor in Γ, and we obtain the asymptotic behavior

$$\bar{l} \approx a_V \left[\frac{u-u_c}{u_c} \right]^{-2} \quad \text{with } u_c(D,T) \approx \frac{\hat{f}_0 D^{2/3}}{\hat{f}_\infty a_V a_\perp^{1/3} \Sigma^{1/3}} , \tag{40}$$

where $\hat{f}(x) \approx \hat{f}_0 x^{1/3}$ has been used. Numerically, the general result $\bar{l} \sim (u-u_c)^{-2}$ could be confirmed over a wide range of T and D values. Some of the data obtained at an intermediate temperature $T=0.5$ are shown in Fig. 8. By extrapolation of these and similar data we find the critical potential strength $u_c(D,T)$. In Fig. 9, u_c is plotted against $D^{2/3}$. For low T, or for large D, we verify $u_c \sim D^{2/3}$ as predicted by (40). For $T=1.0$, the crossover to the high-temperature asymptote $u_c \sim D$ can be seen at least qualitatively. For the dimensionless prefactors, we find the estimate $\hat{f}_0/\hat{f}_\infty \simeq 0.56$.

For a more direct confirmation of our conjecture, we show in Fig. 10 numerical results at $T=0$, plotted against the reduced potential strength $(u-u_c)/u_c$, with the critical potential strength u_c as given by (40).

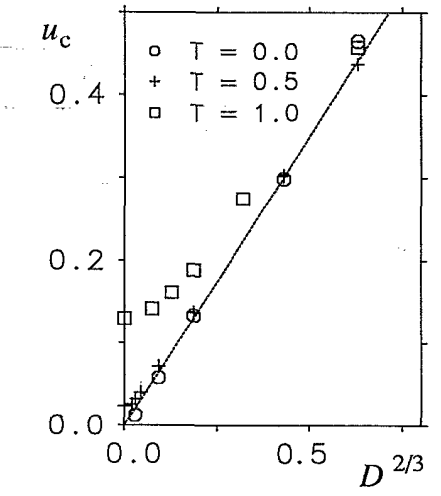

FIG. 9. Critical potential strengths $u_c(D,T)$, as determined by extrapolation from numerical calculations of $\bar{l}(u)$. For small T or large D, $u_c \approx 0.70 D^{2/3}$, as given by the dashed line.

VIII. DELOCALIZATION FROM A SYMMETRIC SQUARE-WELL POTENTIAL

Finally, let us consider an interface in the two-dimensional Ising model which contains a "defect line" of weak bonds. In this case, the interface feels an attractive potential given by

$$V_0(l) = \begin{cases} 0 & \text{for } l \le -a_V/2 \\ -u & \text{for } -a_V/2 < l < a_V/2 \\ 0 & \text{for } a_V/2 \le l \ . \end{cases} \tag{41}$$

In the continuum limit, this potential should belong to the same universality class as the δ function potential $V_0(l) = -u\delta(l)$. Since $\bar{l}=0$ by symmetry, we have to study the second moment $\xi_\perp = (\overline{l^2})^{1/2}$. A finite value of $\xi_\perp$ describes a *localized* interface pinned to the well.

In the absence of frozen disorder, the interface is always localized by the defect line for $u>0$.[13] It is then useful to study the behavior of $V_0(l)$ under the scale transformation given by

$$x \to x/b, \quad l \to l/b^\zeta, \quad \text{and } \mathcal{H} \to \mathcal{H}/b^\chi , \tag{42}$$

which implies $V_0(l) \to b^{\zeta\tau} V_0(b^\zeta l)$ with $\tau = (1-\chi)/\zeta$. For the δ-function potential $V_0(l) = -u\delta(l)$, this implies $u \to b^\lambda u$ with $\lambda = \zeta(\tau - 1)$. In the case of thermally excited interface fluctuations with $\zeta = \frac{1}{2}$, $\tau = 2$, and $\lambda = \frac{1}{2}$, this corresponds to the trivial delocalization fixed point $V_0^*(l) \equiv 0$ and the critical behavior $\xi_\perp \sim u^{-\nu_\perp}$, with $\nu_\perp = \zeta/\lambda = 1$. A random-bond system in $d = 1+1$, on the other hand, represents a marginal case, since $\tau = 1$ and $\lambda = 0$. It is then possible that the delocalization transition

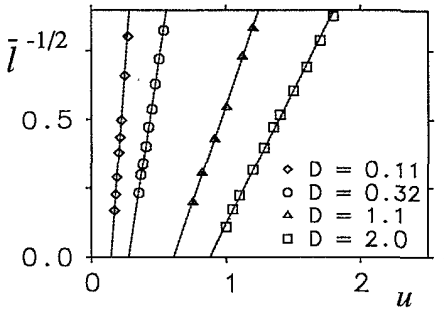

FIG. 8. Interface in the well potential (31) at $T=0.5$ for different D. The behavior $\bar{l} \sim (u-u_c)^{-2}$ is confirmed. The critical potential strengths $u_c(T,D)$ shown in the next figure are obtained by extrapolation of these data to $\bar{l}^{-1/2}=0$.

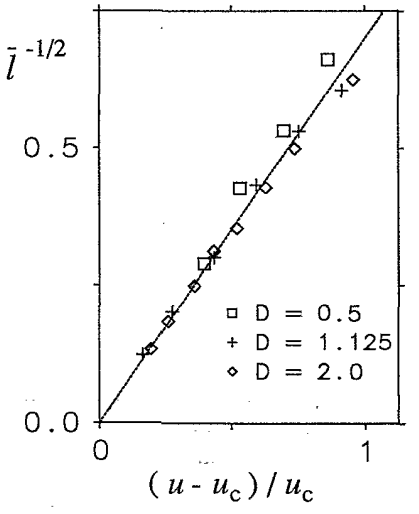

FIG. 10. Interface in the well potential (31) at $T=0$ for different D. The interfacial separation is plotted against the reduced potential $(u-u_c)/u_c$ with u_c as given by (40).

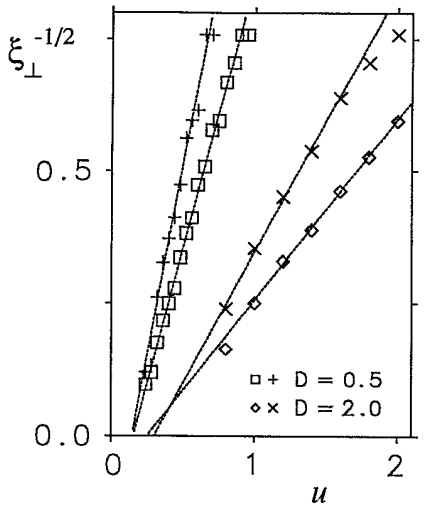

FIG. 11. Pinning of an interface by a line of defects [square-well potential (41) with $a_V=\Delta l$] at $T=0$. The second moments shown are $\xi_{\perp_e}(+,\times)$ and $\xi_{\perp_{av}}(\square,\diamond)$. All data are consistent with $\xi_\perp\sim(u-u_c)^{-2}$ and $u_c>0$.

is given by a nontrivial fixed point $V_0^*(l)$, and occurs at $u=u_c\neq 0$.

Preliminary simulations by Kardar[3] indicated a transition at $u=u_c\neq 0$, with $\xi_\perp\sim(u-u_c)^{-\nu_\perp}$ and $\nu_\perp\simeq 1$. The evaluation of $l(x)$ was, however, restricted to $-30\lesssim l\lesssim 30$, and so the asymptotic regime was not reached.

Here we performed simulations over the range $-1000\leq l\leq 1000$, which implies that $\xi_\perp$ could grow up to $\xi_\perp\simeq 100$. Results at $T=0$ are shown in Fig. 11. The quantity $\xi_\perp^{-1/2}$ has been plotted against u, so that u_c can be determined by extrapolation of this quantity to zero. In these simulations, we have computed not only $\xi_{\perp_e}$ but also $\xi_{\perp_{av}}$ (see Appendix C). Thus the critical potential strengths u_c could be determined by two independent extrapolations. We find $u_c=0.15\pm 0.005$ for $D=0.5$, and $u_c=0.27\pm 0.02$ for $D=2.0$. Thus the interface seems to undergo a nontrivial delocalization transition. The data are consistent with

$$\xi_\perp\sim(u-u_c)^{-\nu_\perp} \text{ and } \nu_\perp=2 . \tag{43}$$

ACKNOWLEDGMENTS

Most of this work was done at the University of Munich. We thank Marc Girardet, Stefan Grotehans, Theo Nieuwenhuizen, and Götz Schmidt for stimulating discussions.

APPENDIX A: SCALING FORMS

In Sec. III, we used scaling forms for the amplitude l_0 in order to estimate various amplitudes and the effective potential acting on the fluctuating interface. Here we show how these scaling forms are obtained in general dimension $d=d_\parallel+1$.

We start from the effective Hamiltonian $\mathcal{H}$ in the form

$$\mathcal{H}\{l(x)\}=\int d^{d_\parallel}x\left[\frac{\tilde{\Sigma}}{2}(\nabla l(x))^2+V_r(x,l(x))\right], \tag{A1}$$

with

$$\langle V_r(x,l)V_r(x',l')\rangle=2D\delta_{a_\parallel}^{d_\parallel}(x-x')\delta_{a_\perp}(l-l') . \tag{A2}$$

The scaling relation found for the interface fluctuations

$$L_\perp\approx l_0^{1-\zeta}L_\parallel^\zeta \tag{A3}$$

suggests that the reduced Hamiltonian $\mathcal{H}/T$ is invariant under the rescaling

$$x\to x/b \text{ and } l\to l/b^\zeta . \tag{A4}$$

Accordingly, the widths of the random potential distribution rescale as $a_\parallel\to a_\parallel/b$ and $a_\parallel\to a_\perp/b^\zeta$. To determine the scaling dimension of the quantities T, D, and $\tilde{\Sigma}$ we introduce reduced variables with the dimension of a length,

$$l_T=(T/\tilde{\Sigma})^{1/d_\parallel} \text{ and } l_D=(D/\tilde{\Sigma}^2)^{1/d} . \tag{A5}$$

From the scale invariance of $\mathcal{H}/T$, we obtain the rescaling

$$l_T\to l_T/b^{(d_\parallel-2+2\zeta)/d_\parallel},\quad l_D\to l_D/b^{(d-5+5\zeta)/d} . \tag{A6}$$

Now, two length scales a_0 and a_1 are defined as $a_i=l_T^{x_i}l_D^{1-x_i}$, and the exponents x_i are chosen to ensure the simple scaling behavior $a_0\to a_0$ and $a_1\to a_1/b^\zeta$. By elementary algebra, one finds

$$a_0=l_T^{(4-5\zeta-d_\parallel)d_\parallel/(3d_\parallel-2)(1-\zeta)}\times l_D^{(-2+2\zeta+d_\parallel)(d_\parallel+1)/(3d_\parallel-2)(1-\zeta)} \tag{A7}$$

and

$$a_1=l_T^{(4-d_\parallel)d_\parallel/(3d_\parallel-2)}l_D^{(d_\parallel-2)(d_\parallel+1)/(3d_\parallel-2)} . \tag{A8}$$

We now proceed to determine a scaling form for the amplitude l_0. As (A3) is valid for different length scales, l_0 has to be invariant under the rescaling (A4). In the absence of a random potential, l_0 can depend on T and $\tilde{\Sigma}$ only. Since $\zeta=(2-d_\parallel)/d_\parallel$ for thermally excited fluctuations, the scale-invariant length a_0 is simply given by $a_0=l_T=T/\tilde{\Sigma}$, and $l_0=f_{\text{th}}T/\tilde{\Sigma}$, where f_{th} is a dimensionless coefficient.

In the presence of frozen randomness, l_0 will depend on the strength D and, in general, on the vertical width $a_\perp$ of the random potential correlator given by (A2). The horizontal width $a_\parallel$, however, should be irrelevant.[14,10] A scale-invariant combination of T, $\tilde{\Sigma}$, D, and $a_\perp$ must then have the form

$$l_0=a_0f(a_1/a_\perp) . \tag{A9}$$

In $d=1+1$ dimensions with $\zeta=\frac{2}{3}$, one has

$$l_0=(D/\tilde{\Sigma}T)f(T^3/D\tilde{\Sigma}a_\perp) . \tag{A10}$$

In the limiting cases of small and large T, the function $f(x)$ is determined up to a dimensionless coefficient: For small T, l_0 must become independent of T, which implies $f(x)\approx f_0 x^{1/3}$ for small x. For large T, on the other hand, the distribution of interface positions is thermally broadened and thus insensitive to the microscopic details of the random potential. In this case l_0 is independent of $a_\perp$, and we have $f(x)\approx f_\infty$ for large x.

APPENDIX B: DERIVATION OF THE SCHRÖDINGER EQUATION

In this appendix, we show under which conditions the recursion

$$W(x+\Delta x,l)=\mathcal{N}^{-1}\sum_{l'}\Delta l\exp\left[-\frac{\Delta x H_x(l,l')}{T}\right]W(x,l')\ , \tag{B1}$$

with

$$H_x(l',l)=\frac{\tilde{\Sigma}}{2}\left[\frac{l'-l}{\Delta x}\right]^2+V(x,l) \tag{B2}$$

may be transformed into a partial differential equation of the Schrödinger type.

If the distribution $W(x,l')$ as a function of l' varies slowly on the scale Δl, it can be expanded into a Taylor series, leading to

$$W(x+\Delta x,l)\approx\mathcal{N}^{-1}\exp\left[-\frac{\Delta x V(x,l)}{T}\right]\times\sum_{l''}\Delta l'\exp\left[-\frac{\tilde{\Sigma}l''^2}{2T\Delta x}+l''\frac{\partial}{\partial l}\right]\times W(x,l)\ . \tag{B3}$$

The dummy variable l'' counts the steps of the interface in the l direction.

At this point, we have to make three different approximations in order to obtain from (B3) a differential equation:

(1) The first approximations is made performing the sum over l'' in one of the two possible limiting cases. In case (i) the variance $(T\Delta x/\tilde{\Sigma})^{1/2}$ of the Gaussian exponential is large compared to the lattice constant Δl. The sum can then be performed as an integral, and one obtains

$$W(x,\Delta x,l)=\mathcal{N}^{-1}\exp\left[-\frac{\Delta x V(x,l)}{T}\right]\times\left[\frac{2\pi T\Delta x}{\tilde{\Sigma}}\right]^{1/2}\exp\left[\frac{T\Delta x}{2\tilde{\Sigma}}\frac{\partial^2}{\partial l^2}\right]W(x,l)\ . \tag{B4}$$

In case (ii), on the other hand, $(T\Delta x/\tilde{\Sigma})^{1/2}$ is small against Δl, so that it is sufficient to consider only jumps by $l''/\Delta l=0,\pm1$ (in the restricted solid-on-solid model, this condition is imposed *a priori*). In this case, the sum can be performed explicitly, leading to

$$W(x+\Delta x,l)=\mathcal{N}^{-1}\exp\left[-\frac{\Delta x V(x,l)}{T}\right]\times\left[1+2\exp\left[-\frac{\tilde{\Sigma}(\Delta l)^2}{2T\Delta x}\right]\times\cosh\left[\Delta l\frac{\partial}{\partial l}\right]\right]W(x,l)\ . \tag{B5}$$

(2) The next approximation consists in retaining only the second-order terms in $\partial/\partial l$. Choosing an appropriate normalization $\mathcal{N}$, we obtain

$$W(x+\Delta x,l)=\exp\left[-\frac{\Delta x V(x,l)}{T}\right]\left[1+\frac{\Delta x}{T}\Gamma\frac{\partial^2}{\partial l^2}\right]\times W(x,l)\ , \tag{B6}$$

with a coefficient Γ that is different in the two limiting cases:

$$\Gamma=\begin{cases}\dfrac{T^2}{2\tilde{\Sigma}} & \text{for case (i)}\\[2ex] \dfrac{T\Delta l^2}{\Delta x}\exp\left[-\dfrac{\tilde{\Sigma}(\Delta l)^2}{2T\Delta x}\right] & \text{for case (ii)}\ .\end{cases} \tag{B7}$$

The range of validity of the second approximation may be estimated by replacing $\partial/\partial l$ by $1/\xi_\perp$. Gathering the conditions for the first and second approximations, one has to require

$$\begin{aligned}&\Delta l\ll(T\Delta x/\tilde{\Sigma})^{1/2}\ll\xi_\perp \quad\text{for case (i)}\ ,\\ &(T\Delta x/\tilde{\Sigma})^{1/2}\ll\Delta l\ll\xi_\perp \quad\text{for case (ii)}\ .\end{aligned} \tag{B8}$$

(3) Finally, the third approximation is made retaining only the first order of the Taylor expansion of $\exp(-\Delta x V/T)$. This leads to

$$W(x+\Delta x,l)=\left[1-\Delta x\left[\frac{V(x,l)}{T}-\frac{\Gamma}{T}\frac{\partial^2}{\partial l^2}\right]\right]W(x,l)\ , \tag{B9}$$

provided $|V(x,l)|\Delta x/T\ll1$. If $W(x,l)$ is smooth as a function of x, (B9) can be written as a Schrödinger equation:

$$\frac{\partial}{\partial x}W_x(l)=-\frac{\hat{H}(x,l)}{T}W_x(l)\ , \tag{B10}$$

with a Hamilton operator

$$\hat{H}(x,l)\equiv V(x,l)-\Gamma\frac{\partial^2}{\partial l^2}\ . \tag{B11}$$

APPENDIX C: NUMERICAL SIMULATIONS

In this appendix, we comment on the algorithms used for the numerical simulations both at $T=0$ and $T>0$. In particular, we explain the different averaging procedures that lead to the mean distance $\bar{l}$ of the interface from the wall.

The first remark is about the very definition of the model. When the lattice is seen as a discretized version of the continuum model, the energy per step in the x direction is given by (24):

$$H_x(l',l)=\frac{\tilde{\Sigma}}{2}\left[\frac{l'-l}{\Delta x}\right]^2+V(x,l)\ . \tag{C1}$$

The original motivation to study random-bond systems, however, came from the Ising model, which leads directly to

$$H_x(l',l)=\frac{J}{2}\left|\frac{l-l'}{\Delta x}\right|+V(x,l)\ . \tag{C2}$$

In the absence of $V(x,l)$, a renormalization of the corresponding transfer matrices[15] shows that (C1) and (C2) belong to the same universality class, the behavior on large scales being given by (C1). Alternatively, one may use the central limit theorem to show that the behavior on large scales is governed by a Gaussian distribution. For numerical purposes, both definitions of $H_x(l,l')$ are equivalent as long as we are in the low-temperature regime with $(T\Delta x/\tilde{\Sigma})^{1/2}\ll\Delta l$, for which most jumps in the l direction are by one lattice constant only and $(l-l')/\Delta l=0,\pm1$.

At $T=0$, the ground state of the interface is given by a path $\{l(x)\}$ of minimal energy. Let $E(x,l)$ be the ground-state energy of an interface running from (0,0) to (x,l). It can be determined recursively by

$$E(x+\Delta x,l)=\min_{l'}\left[H_x(l,l')+E(x,l')\right]\ . \tag{C3}$$

Let $L_\perp$ be the vertical size of the simulated system. At first sight, it might seem necessary to compute $H_x(l,l')+E(x,l')$ for all pairs (l,l'), taking $L_\perp^2$ operations per recursion step. However, if $H_x(l,l')$ is given by (C2), the computational effort can be reduced to $O(L_\perp)$ by an efficient algorithm due to Huse and Henley; see Ref. 11. We performed all simulations at $T=0$ with $H_x(l,l')$ as given by (C2).

The mean interfacial separation $\bar{l}$ can now be determined in two different ways. By averaging over the $l(x)$ that minimize $E(x,l(x))$, we obtain a mean value $\bar{l}_e$ that corresponds to a free boundary condition at the edge $(x,l(x))$. On the other hand, we first calculate a path of minimal energy, $\{l(x)\}$, connecting (0,0) and $(L_\parallel,0)$, and then average $l(x)$ along this path. We then obtain a mean value $\bar{l}_{\rm av}$ that corresponds to an interface segment pinned at the boundaries $x=0$ and $L_\parallel$. As the calculation of $\bar{l}_{\rm av}$ requires considerably more calculation time than that of l_e, we have determined $\bar{l}=l_e$ throughout Secs. IV–VII. In Sec. VIII, results for both mean values are given. As is to be expected, one finds that $\bar{l}_e$ and $\bar{l}_{\rm av}$ exhibit the same critical behavior.

For $T>0$, the interface configurations are governed by the distribution $W(x,l)$. We start from an arbitrary initial distribution, e.g., $W(0,l)=\delta(l)$. Then, we compute $W(x,l)$ by the recursion relation (B1), implemented in the form

$$W(x+\Delta x,l)=\exp\left[-\frac{\Delta x V(x,l)}{T}\right]\times\sum_{l''}\Delta l\exp\left[-\frac{\tilde{\Sigma}l''^2}{2T\Delta x}\right]W(x,l+l'')\ , \tag{C4}$$

with a subsequent normalization step. Again, it is preferable to work in the low-temperature range, where the summation in (C4) has to be performed over a small number of steps l'' only. In this case, the number of operations required by (C4) is again of the order $L_\perp$. Since at $T>0$ there is no computational advantage in using (C2), $H_x(l,l')$ has been simulated as given by (C1). The mean interfacial separation $\bar{l}_e$ is given as an average over the thermal expectation values

$$\langle l(x)\rangle=\sum_l lW(x,l)\Big/\sum_l W(x,l)\ . \tag{C5}$$

We conclude this appendix with an estimate of the computation time needed for one mean value $\bar{l}$. To ensure that $\bar{l}$ is not affected by finite-size effects, we choose a transverse system size of about $L_\perp\simeq10\bar{l}$. In order to determine $\bar{l}$ with an accuracy of 3%, we have to average over 1000 independent realizations of the random potential $V_r(x,l)$, or over 1000 uncorrelated interface segments in a single, large realization of V_r. Interface segments can be regarded as uncorrelated when they are separated by a correlation length $\xi_\parallel$. So we have to average over a system of horizontal size $L_\parallel\simeq1000\xi_\parallel$. According to (8), one has $\xi_\parallel\sim\xi_\perp^{3/2}$, and in all fluctuation regimes the relation $\xi_\perp\sim\bar{l}$ is valid. Thus the total number of operations will be of the order

$$L_\perp L_\parallel\simeq1000\xi_\parallel10\bar{l}\simeq10^4\bar{l}^{5/2}\ . \tag{C6}$$

The strong dependence on $\bar{l}$ explains why our data are restricted to $\bar{l}\lesssim100$.

[1]R. Lipowsky and M. E. Fisher, Phys. Rev. Lett. **56**, 472 (1986); Phys. Rev. B **36**, 2126 (1987).
[2]M. E. Fisher, J. Chem. Soc. Faraday Trans. 2 **82**, 1569 (1986).
[3]M. Kardar, Phys. Rev. Lett. **55**, 2235 (1985); Nucl. Phys. B **290**, 582 (1987).
[4]R. Lipowsky, Phys. Scr. T **29**, 259 (1989).
[5]M. E. Fisher and D. S. Fisher, Phys. Rev. B **25**, 3192 (1982).
[6]Th. Nattermann, Z. Phys. **54**, 247 (1984).
[7]R. Lipowsky, Phys. Rev. Lett. **52**, 1429 (1984); Phys. Rev. B **32**, 1731 (1985).
[8]D. A. Huse and Chr. L. Henley, Phys. Rev. Lett. **54**, 2708 (1985).
[9]D. A. Huse, Chr. L. Henley, and D. S. Fisher, Phys. Rev. Lett. **55**, 2924 (1985).
[10]Th. Nattermann and W. Renz, Phys. Rev. B **38**, 5184 (1988).
[11]M. Huang, M. E. Fisher, and R. Lipowsky, Phys. Rev. B **39**,

2632 (1989).
[12]R. Lipowsky and Th. M. Nieuwenhuizen, J. Phys. A **21**, L89 (1988).
[13]Th. W. Burkhardt, J. Phys. A **14**, L63 (1981).
[14]G. Grinstein and S.-k. Ma, Phys. Rev. Lett. **49**, 685 (1982); Phys. Rev. B **28**, 2588 (1983).
[15]F. Jülicher, R. Lipowsky, and H. Müller-Krumbhaar, Europhys. Lett. **11**, 657 (1990).